Chemistry and Physics of Lipids 221 (2019) 53–64

Contents lists available at ScienceDirect

Chemistry and Physics of Lipids

journal homepage: www.elsevier.com/locate/chemphyslip

Sulfate-based lipids: Analysis of healthy human fluids and cell extracts

Irundika H.K. Dias[a], Rita Ferreira[b], Florian Gruber[c,d], Rui Vitorino[e,f], Andrea Rivas-Urbina[g], José Luis Sanchez-Quesada[g], Joana Vieira Silva[f,h,i], Margarida Fardilha[f], Victor de Freitas[j], Ana Reis[j,*]

[a] Aston Medical School, Aston University, Birmingham, B4 7ET, UK
[b] Departamento de Química, Research Unit of Química Orgânica, Produtos Naturais e Agro-alimentares (QOPNA), Universidade de Aveiro, 3810-193, Aveiro, Portugal
[c] Medical University of Vienna, Department of Dermatology, Vienna, Austria
[d] Christian Doppler Laboratory for Biotechnology of Skin Aging, Vienna, Austria
[e] Unidade de Investigação Cardiovascular, Departamento de Cirurgia e Fisiologia, Faculdade de Medicina, Universidade do Porto, 4200-319, Porto, Portugal
[f] Department of Medical Sciences, Institute of Biomedicine – iBiMED, University of Aveiro, 3810-193, Aveiro, Portugal
[g] Cardiovascular Biochemistry, Biomedical Research Institute IIB Sant Pau, Sant Antoni Ma Claret, 167, Barcelona, Spain
[h] Reproductive Genetics & Embryo-fetal Development Group, Institute for Innovation and Health Research (I3S), University of Porto, Porto, Portugal
[i] Unit for Multidisciplinary Research in Biomedicine (UMIB), Institute of Biomedical Sciences Abel Salazar (ICBAS), University of Porto, Porto, Portugal
[j] LAQV/REQUIMTE, Departamento de Química e Bioquímica, Faculdade de Ciências, Universidade do Porto, Rua do Campo Alegre 687, 4169-007, Porto, Portugal

ARTICLE INFO

Keywords:
Cholesterol sulfate
Sulfoglycolipids
Taurine conjugates
Seminal fluid
Electronegative LDL
Polyphenol metabolites
Hypurate conjugates

ABSTRACT

Sulfate-based lipids (SL) have been proposed as players in inflammation, immunity and infection. In spite of the many biochemical processes linked to SL, analysis on this class of lipids has only focused on specific SL subclasses in individual fluids or cells leaving a range of additional SL in other biological samples unaccounted for.

This study describes the mass spectrometry screening of SL in lipid extracts of human fluids (saliva, plasma, urine, seminal fluid) and primary human cells (RBC, neutrophils, fibroblasts and skin epidermal) using targeted precursor ion scanning (PIS) approach. The PIS 97 mass spectra reveal a wide diversity of SL including steroid sulfates, sulfoglycolipids and other unidentified SL, as well as metabolites such as taurines, sulfated polyphenols and hypurate conjugates. Semi-quantification of SL revealed that plasma exhibited the highest content of SL whereas seminal fluid and epithelial cells contained the highest sulphur to phosphorous (S/P) ratio.

The complexity of biofluids and cells sulfateome presented in this study highlight the importance of expanding the panel of synthetic sulfate-based lipid standards. Also, the heterogenous distribution of SL provides evidence for the interplay of sulfotransferases/sulfatases, opening new avenues for biomarker discovery in oral health, cardiovascular, fertility and dermatology research areas.

1. Introduction

The advent of soft ionisation techniques in the 1980´s (Fenn et al., 1989; Karas et al., 1987) was pivotal in the analysis of high molecular weight biomolecules with low thermal stability by Mass Spectrometry (MS). In recent years, the development of user-friendly instruments has greatly contributed to the increasingly popularity of MS in the screening, characterization and quantification of lipids (Gruber et al., 2007; Hammond et al., 2012; Hart et al., 2011; Kompauer et al., 2017; Leitinger et al., 1999; Maciel et al., 2014; Schuhmann et al., 2012; Stübiger et al., 2012) which associated with the high mass range, high sensitivity, and fast scan rates makes MS ideally suitable for the high-throughput analysis of lipids in complex biological samples (Garwolińska et al., 2017; Kosinska et al., 2013; Larsson et al., 1996; Pizarro et al., 2013) particularly in the detection of less abundant lipids, such as sulfolipids.

Sulfolipids are a heterogenous class of lipids containing sulfur atom in its structure (Farooqui and Horrocks, 1985; Goldberg, 1961) present in its oxidised state as sulfate-based lipids (SL) and sulfonate-based lipids, or in its reduced state as thioether or thiol ester compounds linked to acyl chains with amino acids. SL appear to be ubiquitous to the whole body and dispersed across fluids (Lam et al., 2014; Larsson et al.,

Abbreviations: CE, collision energy; EPI, enhanced production; LLE, liquid-liquid extraction; NAT, n-acyl taurines; PIS, product ion scanning; Pi, inorganic phosphate; RBC, red blood cells; R.A., relative abundance; SL, sulfate-based lipids; SGC, sulfogalacto-ceramides; DHEA, dehydroepiandrosterone; NEFA, non-esterified fatty acids

* Corresponding author at: Rua do Campo Alegre 687, 4169-007, Porto, Portugal.
E-mail address: anpereira@fc.up.pt (A. Reis).

https://doi.org/10.1016/j.chemphyslip.2019.03.009
Received 26 November 2018; Received in revised form 15 March 2019; Accepted 15 March 2019
Available online 22 March 2019

1996; Lee et al., 2016; Muskiet et al., 1983; Sion et al., 2001; Yao et al., 2016) and tissues (Cho et al., 2010; Fujimoto et al., 2000; Moyano et al., 2014; Seng et al., 2014; Serizawa et al., 1990). SL are catalysed by a supergene family of enzymes called sulfotransferases (SULTs) with the transfer of a sulfuryl group (SO_3-) to an acceptor hydroxyl group resulting in an increase of water solubility and decrease of biological activity and at the cellular level, SL appear to be gathered in lipid-raft domains (Weerachatyanukul et al., 2007) at the surface of cells (Honke, 2018) contributing to membrane´s electronegative surface charge at physiological pH and thus involved in cell-cell communication processes (Farooqui and Horrocks, 1985; Honke, 2018; Strott and Higashi, 2003) in inflammation (Hu et al., 2007), immunity (Avila et al., 1996; Merten et al., 2001) and infection (Suzuki et al., 2003). The identification of SL-rich microenvironments conducted by MS tissue imaging studies in cancerous tissues (Eberlin et al., 2010; Liu et al., 2010; Masterson et al., 2011), and the recently reported role of SULT enzymatic systems in proper lipoproteins clearance (Stanford et al., 2010) and the detoxification of deleterious oxysterols (Fuda et al., 2007) hints for the possible de-regulation of SL in disease.

Despite their occurrence in apparently most fluids and tissues, research on SL is scarce and mostly focused on steroid sulfates (Cho et al., 2010; Eberlin et al., 2010; Esquivel et al., 2018; Lafaye et al., 2004; Lam et al., 2014; Lee et al., 2016; Przybylska et al., 1995; Sánchez-Guijo et al., 2015; Sion et al., 2001; Wang et al., 2018; Yao et al., 2016) due to the relevance of steroid sulfates in sports and anti-doping areas, while SL bearing a glycerol-backbone and a sphingosine-backbone (Scheme 1) remain less studied (Mirzaian et al., 2015; Slomiany et al., 1978). Due to the SL structural diversity, analysis of SL in complex biological samples is not straightforward limiting the exploitation of SL diagnostic and prognostic value. In addition to this, researchers employ a variety of solid-phase extraction (SPE) (Fong et al., 2013; Sánchez-Guijo et al., 2015; Wang et al., 2018) or liquid-liquid extraction approaches (LLE) (Kongmanas et al., 2010; Lam et al., 2014; Mirzaian et al., 2015; Sion et al., 2001; Yao et al., 2016), with various solvent systems, and ESI and MALDI ionisation techniques (Serna et al., 2015; Teubel et al., 2018; Wang et al., 2018) which makes comparison of results difficult because of the potential sample losses, the differences in extraction performances and the ionization efficiencies associated with the different approaches (Lee et al., 2014; Pizarro et al., 2013; Reis et al., 2013; Sarafian et al., 2014).

Using the targeted precursor ion scanning approach for sulfate groups (PIS 97), this work aims to optimize the experimental parameters and to simultaneously screen the low and high molecular weight SL in lipid extracts obtained in a range of non-invasive (or minimally invasive) biological fluids and cells collected in laboratories across Europe. To achieve this, lipid extracts were prepared using the same extraction procedure and injected phospholipid amount into the MS injection in order to facilitate the comparison and estimates on the sulphur-to-phosphorous ratio in fluids and cells. Additional diagnostic fragment was included to improved confidence on SL identification.

2. Material and methods

2.1. Reagents

Synthetic lipids (DHEA and d18:1/17:0 sulfatide) were purchased from AVANTI Polar Lipids (Alabaster, USA). All chemicals used in sample preparation, isolation, purification and quantification were of analytical grade or the highest purity commercially available. Sodium molybdate ($NaMoO_4.H_2O$), sodium dihydrogenophosphate (NaH_2PO_4), perchloric acid (70%, $HClO_4$) and ascorbic acid were from Sigma. PBS tablets used in lipoprotein desalting dialysis were purchased from Sigma. All organic solvents were of HPLC grade or the highest purity commercially available (Fisher Scientific, Leicester, UK). Milli-Q water was filtered through a 0.22 µm filter system (Milli-Q plus 185, Millipore).

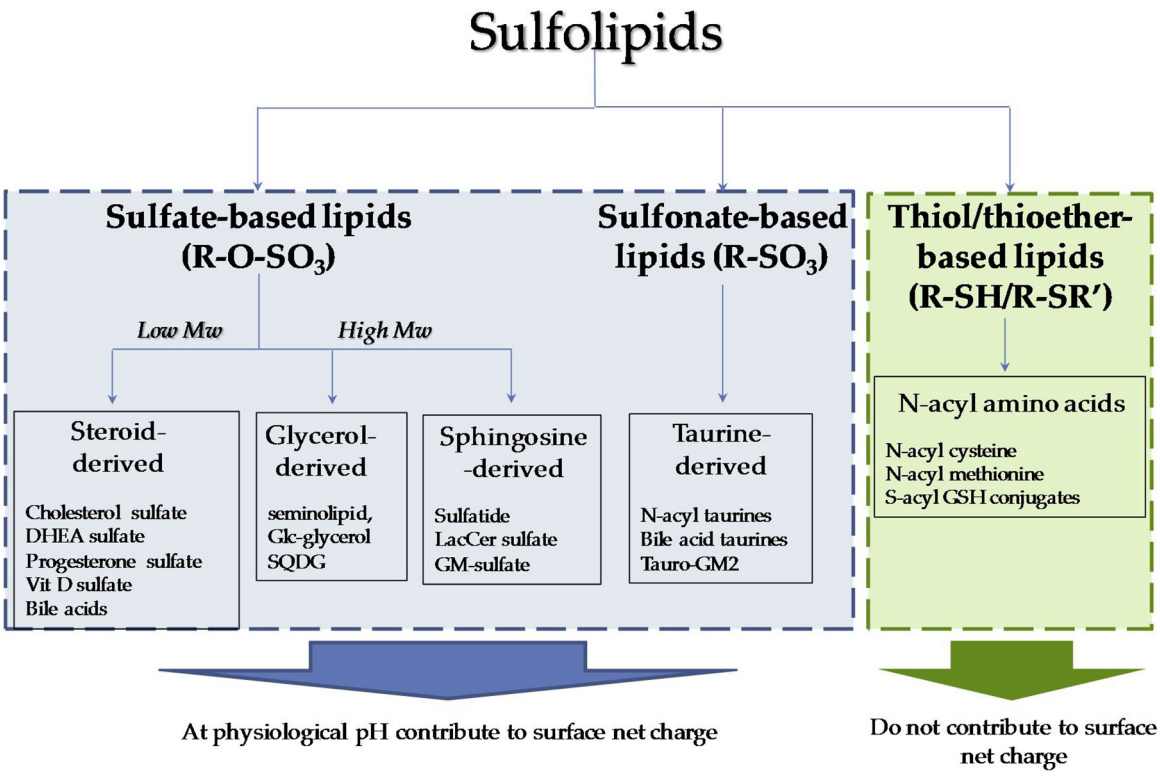

Scheme 1. Scheme depicting sulfolipid sub-classes categorized in its oxidised state (sulfate- and sulfonate-based lipids) and its reduced state form (thiol/thioether-based lipids). Sulfate-based lipids (SL) comprising low and high molecular weight are further categorised in steroid-derived, glycerol-derived and sphingosine-derived lipids. Sulfate- and sulfonate-based lipids (in blue shaded box) contribute to surface negative charge at physiological pH while thiol and thioether lipid classes (in green shaded box) do not contribute to negative surface charge.

2.2. Biological samples

The study was approved by Local Ethics Committee and conducted in accordance to the ethical standards of the Declaration of Helsinki. Human fluid and cell samples were collected from healthy donors who gave written informed consent prior to participation in this study. Additional information regarding the donors, sample collection, and purification procedures prior to the analysis of lipid extracts is detailed below.

2.2.1. Human fluid samples

Saliva samples were collected from 2 healthy male donors, aged 25 ± 5 years, and showing no evidence of oral pathologies, inflammation or caries. Donors, refrained from eating and drinking in the previous 2 h, donated unstimulated saliva by direct draining into a sterile saliva collection tube. Saliva samples were pooled and processed by centrifugation at 14,000x*g* at 4 °C for 15 min, and kept in freezer (−80 °C) until further analysis. Plasma sample was obtained from venous blood collected from one healthy male donor aged 30 into EDTA Vacutainer tubes and centrifuged at low speed (600x*g*, 15 min). Plasma (upper phase) was separated and stored in the freezer until further use. Urine samples from 2 healthy male donors, aged 25 ± 5 (BMI < 25) were collected into sterile Falcon tubes and processed by centrifugation for 10 min at 4000x*g* at 4 °C, pooled and kept in freezer until further use. Seminal fluid pooled samples collected from 3 male donors aged 20–25 (BMI < 25) were processed by centrifugation (12,000x*g*, 30 min) for spermatozoa precipitation. The supernatant seminal fluid was aliquoted into eppendorf tubes and kept in the freezer (−80 °C) until further analysis. Purity of seminal fluid was confirmed by the absence of sperm cells using a Zeiss Primo Star microscope (Carl Zeiss AG, Germany). Low density lipoproteins (LDL) were collected from a plasma pool of 10 normolipidemic donors (4 male/6 female) aged 36 ± 8 years and separated by low speed centrifugation (600x*g*, 15 min) and used for lipoprotein isolation. Low-density lipoproteins (LDL) isolated by salt (KBr) gradient ultracentrifugation (density range 1.019–1.050 g/mL) were fractionated in native LDL (LDL(+)) and electronegative LDL (LDL(-)) by stepwise anion exchange chromatography as described elsewhere (Bancells et al., 2010). Purity of isolated lipoproteins sub-populations was confirmed by agarose electrophoresis and protein and phospholipid content determined by commercial methods adapted to a Cobas 600/501c autoanalyzer. Protein and phospholipid content were similar in both LDL sub-populations (0.5 g/L and 0.73 mM, respectively). Native and electronegative LDL sub-populations were dialyzed in Slide-A-Lyzer dialysis cassettes (Thermo Scientific, cut-off below 3,5 kDa) against PBS solution (Sigma) before lipid extraction.

2.2.2. Isolation of human cells

One millilitre (1 mL) of venous whole blood collected from a healthy male donor aged 30 into EDTA Vacutainer tubes was transferred into an eppendorf tube and centrifuged at low speed (600x*g*, 15 min). Red blood cells (200 µL) were collected from bottom layer. Peripheral blood neutrophils were isolated using Percoll density centrifugation (Sigma-Aldrich, Poole, UK) according to previously described procedure by Matthews et al. (Matthews et al., 2007). Primary human dermal fibroblasts (neonatal, male foreskin) were obtained from Cascade Biologics (Portland, OR). Human epidermal keratinocytes were isolated from female donors aged 37 to 52 years old according to the previously described protocol (Gruber et al., 2012). This study was approved by the local ethics committee and conducted in accordance with the Declaration of Helsinki principles. Participants gave their written informed consent (EK Nr. 2011/1149).

2.3. Lipid extraction and phospholipid quantification protocols

Lipids from human fluids and cells were extracted by the Folch protocol (Folch et al., 1957) using 0.2–4.0 mL of volume depending on the biofluid and from 1×10^6 cells for neutrophils and keratinocytes, and 1.8×10^6 cells for fibroblast. Extraction was done in glass tubes and repeated twice, organic extracts were combined in glass tubes and evaporated to dryness under nitrogen stream in ice bath. Phospholipid content of lipid extracts was determined (in triplicate) by spectrophotometry measurement of inorganic phosphorous ($\lambda = 797$ nm) using a micromethod adapted from Rouser et al. (Rouser et al., 1970), as described elsewhere (Sousa et al., 2016). Quantification of inorganic phosphorous (Pi) in lipid extracts was done in triplicates against a calibration curve showing a linear range between 0 and 2 µg of Pi ($y = 0.7738x + 0.063$, r^2 0.9989) and phospholipid content in extracts estimated by multiplying by a factor of 25. The spectrophotometric method is widely used to estimate on the total amount of phosphate-containing lipids including phospholipids, cardiolipin and sphingomyelins, whereas lipids without phosphate group, including free fatty acids, cholesterol (free and bound), acylglycerols, and sphingolipids (ceramides, sulfatides, hexosylceramides, lactosylceramides, and gangliosides) are excluded from the estimated value.

2.4. Screening of sulfate-based lipids in lipid extracts by targeted mass spectrometry

Prior to MS analysis, lipid extracts were resuspended in $CHCl_3$:MeOH (1:1, v/v) and normalized to a final concentration of 25 ng phospholipid per microliter (See Optimization of Analysis Conditions Section). Screening of human fluid and cell lipids extracts was conducted by mass spectrometry in a 5500 QTrap instrument (ABSciex, Warrington, UK) operating in the negative ion detection mode over the mass range of 350–1000 Da with direct infusion at a flow rate of 10 µL min^{-1}. Turbo spray source temperature was set at 150 °C, spray voltage of -4.5 kV with declustering potential at −50 eV and nominal curtain gas flow set at 20. Detection of SL in lipid extracts was achieved by targeted detection of precursor ion scanning (PIS) at *m/z* 97.0 collected at 1000 Da/s scan speed with step size of 0.1 Da. Collisional energy employed for the detection of low and high mass range SL was set to −80 eV with Q1 and Q3 set to unit resolution. Enhanced product ion (EPI) spectra were acquired for the ion of interest with Q1 set to low resolution at 10,000 Da/s with collision energy varying between −10 and −100 eV. Dynamic fill time was used with a maximum fill time of 250 ms and all other parameters optimized to give maximum signal. Blank injections were included between samples.

2.5. SL and metabolite identification workflow

SL and other sulfated metabolites observed in the PIS 97 mass spectra were identified through the online databases available including the Human Metabolome Database (HMDB, www.hmdb.com), LipidMaps (www.lipidmaps.com), the Food Component Database (FooDB, www.foodb.ca) and the PhytoHub (www.phytohub.eu). Confirmation of metabolite hits retrieved from database search were confirmed using fragmentation pattern acquired during enhanced product ion (EPI) experiments and cross-referenced with fragmentation patterns (MS/MS data) published in the literature (Hofmann et al., 2016; Kongmanas et al., 2010; Sasso et al., 2016; Satoh Née Okihara et al., 2014).

2.6. Semi-quantification of SL in human biofluid and primary cell extracts

Biofluids and cell extracts screened (in triplicate) by PIS 97 acquisition method and used to estimate SL content in lipid extracts. Peak intensity (cps) for individual ions were obtained from a 2 min time window using the “Data and Peak Table” feature in PeakView software (Analyst, v 1.0.0.6). Peak intensity values were plotted in. xls file for semi-quantification of SL in extracts. Cal curves acquired for low- and high mass SL were built using peak intensities over a 2 min time period

and showed linearity in the 0–150 nM range for DHEA sulfate ($y = 4650.2x + 1354.1$, $r^2 = 0.9997$) and in the 0–60 nM range for d18:1/17:0 sulfatide ($y = 355.95x + 358.73$, $r^2 = 0.9988$). The intra- and inter-day variability was below 5 and 10%, respectively.

3. Results

3.1. Optimization of SL analysis and detection conditions

Precursor ion scanning (PIS) detection approaches rely on the formation of a specific target fragment in the gas-phase for its detection. The formation of the target fragment with high intensity is dependent on several parameters including the collision energy (CE) applied (optimum collision energy) to induce its formation in the gas-phase conditions. The value of the CE is in turn dependent on the molecular mass of the ion of interest. Typically, higher molecular weight compounds require higher collisional energies. Considering SL occur in a wide mass range, from low molecular weight (e.g. steroid sulfates) to high molecular weight (e.g. sulfoglycolipids) (Scheme 1) and in a wide concentration range, likely to impact the optimum collision energy, the partition in organic solvents and the ability to be detected in MS methods, we present data on the optimization of experimental conditions influencing SL analysis.

Collisional fragmentation of synthetic DHEA sulfate (*m/z* 367.1) with collision energy −40 eV shows one product ion at *m/z* 97.0 (Supplemental Figure S1) attributed to HSO_4^-. At CE −50 eV DHEA precursor ion (*m/z* 367.1) completely fragments to the fragment at *m/z* 97 showing its highest intensity (maximum of R.A. %). Plot of the R.A. of fragment at *m/z* 97 in the enhanced product ion (EPI) spectrum increases with increasing CE (Fig. 1A). However, at higher CE > −80 eV the intensity of fragment at *m/z* 97 slightly decays though fragment remains the most abundant in the EPI mass spectra (Fig. 1A). Fragmentation of sulfatide precursor ion ($[M-H]^-$, *m/z* 792.9) at CE −50 eV shows the fragment at *m/z* 97 with residual R.A. (< 1%) displaying its maximum R.A. at CE of −90 eV. The results obtained show that for both standards (DHEA and SGC) the R.A. of diagnostic fragment (*m/z* 97) increases with increasing collisional energy (Fig. 1A) but with different optimum values. At the same time, results shown also evidence that at CE of −50 eV sulfatides and other high molecular weight SL would not generate fragment at *m/z* 97 and hence would not be detected through PIS 97 acquisition method.

In view of the results, the optimum collision energy selected for the precursor ion scanning (PIS) acquisition method was set to an intermediate value (−80 eV). The PIS 97 mass spectrum obtained for the equimolar mixture of SL (shown in Fig. 1B) using the adopted CE (−80 eV) shows that sulfatides are not as easily ionisable when compared to low Mw steroid sulfates. In addition to this, enhanced product ion (EPI) spectra obtained for DHEA and SGC (Supplemental Figure S1) do not show the fragment formed by loss of 80 Da (-SO_3) from precursor ion ($[M-H-80]^-$) suggesting that neutral loss scan (NLS) approaches are a less sensitive approach for the identification of sulfate-based lipids in QTrap instruments.

The quality of mass spectra is equally influenced by the amount of lipids present in the lipid extract and therefore dependent on the performance of the solvent mixture in the liquid-liquid extraction (LLE) step. Experimental data on the extraction efficiency of sulfolipids in 5 different solvent systems (Reis et al., unpublished data) shows that the Folch method (MeOH:$CHCl_3$; 1:2, v/v) and acidified Bligh and Dyer method (MeOH:$CHCl_3$; 2:1, v/v) exhibited the best extraction performances compared to other solvent systems. These organic solvent systems were only partially effective towards the extraction of higher molecular weight sulfatides (Reis et al., unpublished data). In this study, we implemented LLE extraction procedure using a binary solvent system (Folch et al., 1957) for fluids and cells due to its performance, simplicity and popularity in lipidomic studies of fluids and cells (Lee et al., 2014; Sarafian et al., 2014).

Given the panel of biological samples included in this study, and associated differences in water, protein and lipid content, one crucial step is to determine the minimum amount of sample to use without limiting the detection of SL. As all samples underwent the same LLE protocol (Folch protocol), the amount injected into the MS instrument was normalized to a fixed amount of phospholipids. In a test injection, the PIS 97 mass spectra of plasma extracts with different dilution factors (Fig. 2) shows an increase in absolute ion intensity with increase amount injected attributed to increased content of sulfate-based lipids. The ideal dilution factor is always a compromise, and should not be too high to prevent detection or too low to saturate ion intensity resulting in loss of resolution. The biological samples used in this study were diluted to 25 ng PL/μL. The mass range selected between *m/z* 350–1000 excludes the detection of low MW metabolites (< 350 Da) which could lead to peak saturation and ion suppression effects.

3.2. Profile of SL in human fluids and cell extracts

Direct injection of fluid and cells extracts collected from healthy individuals and analysed by PIS 97 targeted detection (depicted in Fig. 3) exhibit a distinct ion profile particularly noticeable at higher mass range for saliva and urine (inserts in Fig. 3). The PIS mass spectra

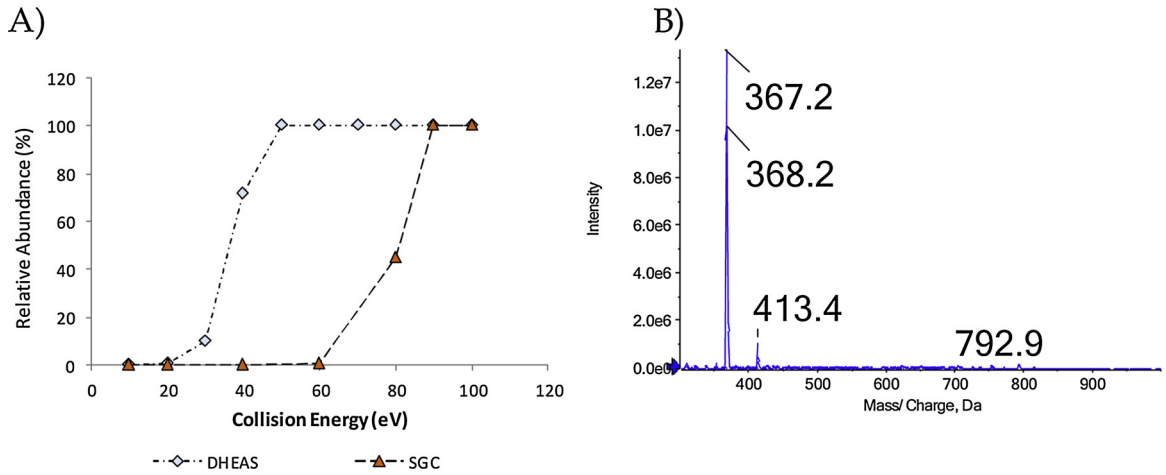

Fig. 1. Optimisation of collision energies (CE) in precursor ion scanning (PIS) method for sulfate-based lipids (A) plot of fragment at *m/z* 97.0 relative abundance (R.A, %) versus collision energy (eV) for DHEA sulfate (diamonds) and sulfogalactosyl-ceramide (triangles). (B) PIS 97 mass spectrum of equimolar mixture of DHEA sulfate (*m/z* 367.1) and sulfogalactosyl-ceramide (d18:1/17:0, *m/z* 792.9) using CE −80 eV. Ion at *m/z* 413.4 is a solvent contaminant.

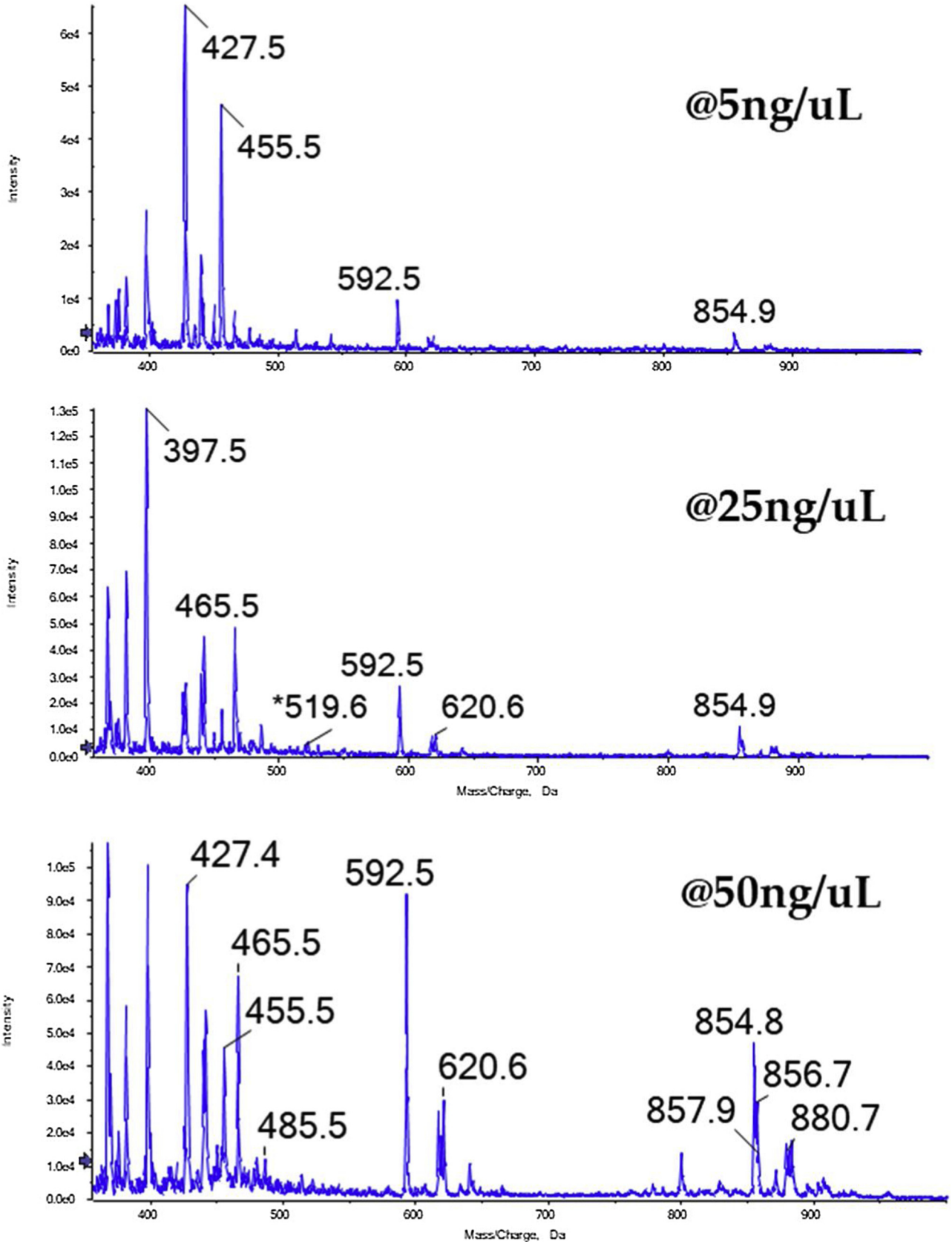

Fig. 2. PIS 97 mass spectra of plasma lipid extracts using different dilution factors obtained by injecting different amounts of phospholipid per volume of solvent (ng PL/μL).

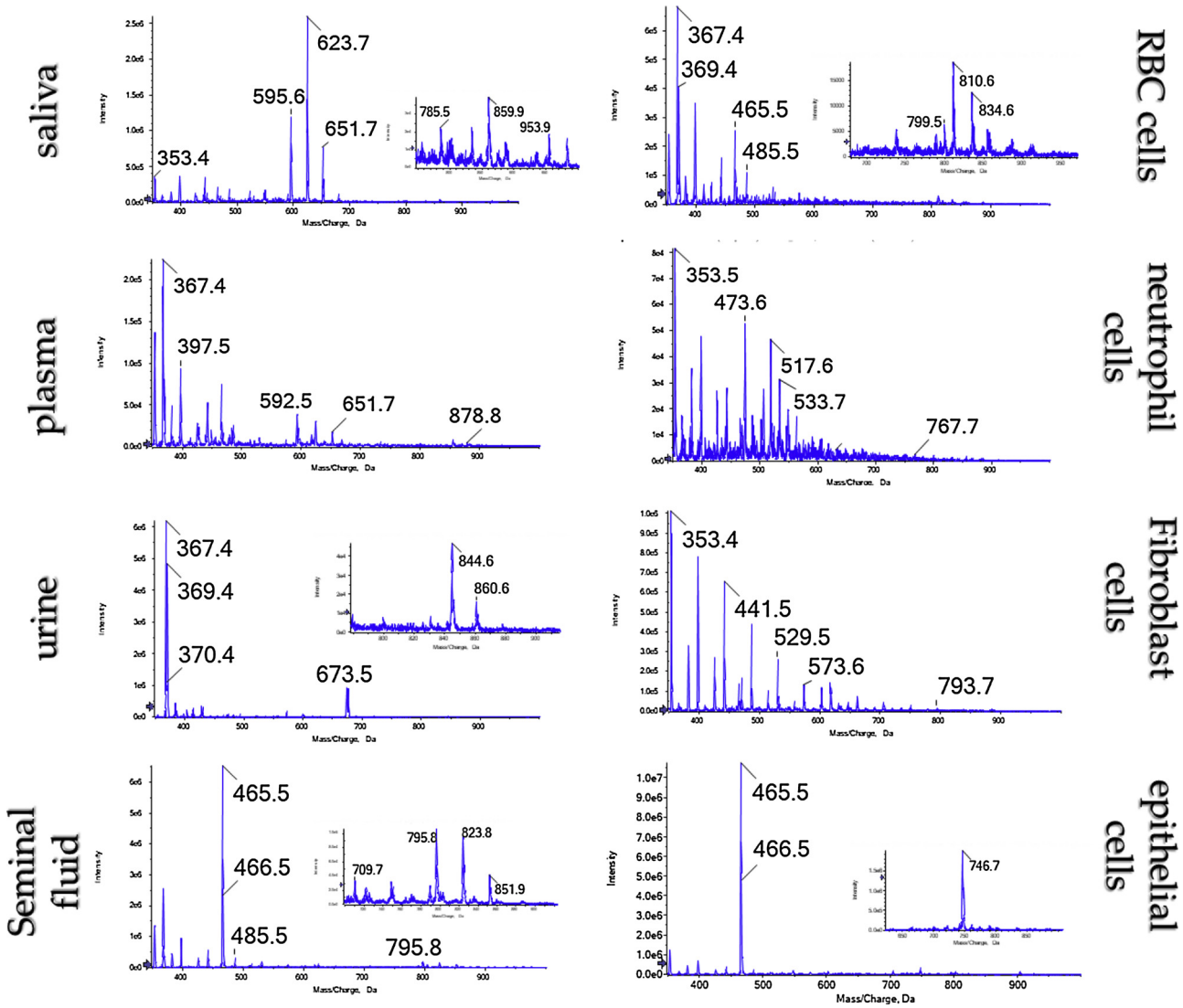

Fig. 3. PIS 97 mass spectra of human biofluids (left-hand panel) and cell lipid extracts (right hand-panel) prepared by the liquid-liquid extraction using Folch solvent system and diluted to 25 ng PL/μL. Insets in figures correspond to zoomed regions of PIS 97 mass spectra.

of native LDL(+) and electronegative low density lipoproteins LDL(-) lipid extracts exhibit similar profile for both sub-populations. Extracts of blood cells (RBC and neutrophils) exhibited mainly low molecular weight sulfate-based lipids (Fig. 3). Identification of SL was mainly achieved through database search (Experimental Section) revealing the presence of several sulfate-based lipids ($[M\text{-}H]^-$ ions) including sulfated steroids and sulfoglycolipids. In view of the scarcity of synthetic standards, confirmation was achieved through fragmentation patterns in EPI mass spectra cross-referenced with available literature (Kongmanas et al., 2010; Sasso et al., 2016; Satoh Née Okihara et al., 2014). In general, SL exhibit abundant product ion at *m/z* 97.0 (base peak) (Mirzaian et al., 2015b) in the negative ion mode. However, as phosphate-based compounds also generate fragments at *m/z* 97 under gas-phase induced fragmentations (Metzger et al., 1995) the signature pair of fragments at *m/z* 97/80 exhibited by sulfated lipids (Supplemental Figure S3) distinct from phosphate-based lipids as these exhibit the pair at *m/z* 97/79 (Metzger et al., 1995) was used to exclude the contribution of false positives. The SL signature fragments can be advantageously used as an additional screening criterion increasing the confidence in compound identification and reducing the inclusion of false positives. Sulfoglycolipids may exhibit additional fragments formed by neutral losses of acyl chains from the $[M\text{-}H]^-$ precursor ion (Goto-Inoue et al., 2009; Kongmanas et al., 2010).

Using the diagnostic signature of SL (Supplemental Figure S3), the SL ions detected in lipid extracts of biological samples are listed in Table 1. All samples exhibited the presence of CholS (*m/z* 465.5) which was particularly intense in seminal fluid, whereas plasma and urine extracts were rich in steroid sulfates. Ions observed in PIS mass spectrum of saliva at *m/z* 803.8, 859.9, 885.9, 887.9, 953.9 and 981.9 (Table 1) were assigned as sulfated glycolipids based on the *m/z* value of previously proposed sulfated salivary lipids (Slomiany et al., 1983, 1978) and on the presence of ion pair *m/z* 97/80 and 256 Da neutral losses from precursor ion in EPI mass spectra. Ions attributed to sulfate-based lipids as well as other unidentified sulfate-based lipids are listed in Table 1.

Other ions observed with low R.A. at *m/z* 418.4, 446.4, 474.4, and 490.4 in the PIS 97 mass spectra of plasma and neutrophils extracts were attributed to N-acyl taurine lipids (Supplemental Table S1) based on the signature fragments of sulfonate-based compounds at *m/z* 124, 107 and 80 (Sasso et al., 2016; Satoh Née Okihara et al., 2014) and a distinct ratio of signature fragments (Supplemental Figure S3). Bearing in mind the SL signature fragments, several other ions were identified as sulfate-based lipids though its structure was not entirely deciphered. For instance, ions observed in saliva´s PIS 97 mass spectrum in the high mass range namely at *m/z* 802.8 (Supplementary Figure S4) and 972.6 exhibited the sulfate signature fragments (*m/z* 97/80) and fragment at

Table 1
List of $[M-H]^-$ ions observed in PIS 97 mass spectra of human fluid and cell lipid extracts corresponding to sulfate-based lipids. Identification was proposed based on hits retrieved by open-source databases (see Experimental Section) and confirmation was achieved by the presence of signature fragments in EPI mass spectra and matching published literature. Fragment ions observed in enhanced product ion spectra (R.A. > 10%) in unidentified sulfate-based lipid is also included.

Ion (m/z value)	Sample	Lipid ID	MSMS spectrum (R.A.,%)
353.3	S	Androstenol sulfate	
365.2	LDL(+)	Hydroxy estrone sulfate	
367.3	P, SF, RBC	DHEA sulfate	
367.3	U	Testosterone sulfate	
369.3	P, RBC, SF, U	Epiandrosterone sulfate	
381.3	S, P, SF, Fb, Nt	Methoxy-estradiol sulfate;	
383.3	LDL(+)	dihydroxyandrostenone sulfate	
397.4	S, P, SF, Nt, Fb,	Pregnanolone sulfate	
425.4	P, LDL(-), RBC, Epi, Fb	Costicosterone sulfate	
429.4	U	Ptilosteroid B	
441.4	P, LDL(+), LDL(-), RBC, Fb,	Cortisol sulfate	
465.3	S; P; U; SF; Epi; RBC; LDL(+), LDL(-)	Cholesterol sulfate	
473.4	U	trihydroxy-5alpha-cholan-24-yl sulfate	
479.3	P	Oxysterol sulfate	
543.4	SF	β-estradiol 3-(β-D-glucuronide) 17-sulfate	
746.7	Epi	ni	79.9 (10), 97.0 (90), 255.3 (10), 438.4 (30), 465.3 (100), 700.5 (10)
769.6	SF	Seminolipid (30:1)	
795.8	SF	Seminolipid (32:0)	
799.8*	S	Sulfoglycolipid I (33:5)	
801.8*	S	Sulfoglycolipid I (33:4)	
802.7	S	ni	96.9 (100), 255.3 (10), 265.3 (100), 293.3 (50), 321. 3 (10), 465.3 (12), 546.4 (3)
803.8*	S	Sulfoglycolipid I (33:3)	
823.8	SF	Seminolipid (34:0)	
851.9	SF	Seminolipid (36:0)	
859.9*	S	Sulfoglycolipid I (37:3)	
885.9*	S	Sulfoglycolipid I (39:4)	
887.9*	S	Sulfoglycolipid I (39:3)	
953.9*	S	Sulfoglycolipid II (32:2)	
972.7	S	ni	79.9 (5), 96.9 (25), 255.3 (35), 265.2 (100), 293.3 (82), 321.4 (20), 465.3 (5), 618.4 (< 5), 716.5 (< 5)
981.9*	S	Sulfoglycolipid II (34:2)	

S: saliva; P: plasma; U: urine; SF: seminal fluid; Nt: neutrophils; RBC: red blood cells; Fb: Fibroblast cells; Epi: epidermal keratinocyte cells; LDL (+): native low density lipoproteins; LDL(-): electronegative low density lipoproteins.
ni: not identified; (C,n) numbers in curve brackets mean number of carbon atoms:number of double bonds.
* Structures of salivary sulfoglycolipids are proposed based on work by Slomiany and colleagues (1978; 1980).

m/z 255.2 together with neutral losses of 256 Da from precursor typically associated to palmitoyl-containing lipids. Ions observed in saliva PIS 97 spectrum at *m/z* 595.5, 623.5 (Supplementary Figure S4) and 651.5 exhibited the signature fragments (*m/z* 97/80) and fragments at *m/z* 265.2 with high R.A (~50%). Ions observed for urine extracts in the high mass range at *m/z* 673.5, 675.5, 844.6 (Supplementary Figure S4) and 860.6 exhibited the signature fragments (*m/z* 97/80), fragments at *m/z* 255.2 typically assigned to palmitoyl carboxylate anion (Hsu and Turk, 2003). Ions at *m/z* 673.5, 675.5, 844.6 and 860.6 exhibited neutral losses of 306 Da from precursor ion, and ions with *m/z* 844.5 and 860.6 exhibited the fragment at *m/z* 178.1 consistent with hypurate-conjugates (Wijeyesekera et al., 2012). Other sulfate-based compounds detected in PIS 97 mass spectra of fluid and cell extracts included sulfated polyphenol (PP) metabolites (Supplemental Table S1). In addition to these, PIS 97 mass spectra also showed the presence of phosphate-based lipids (phospholipids) including serine-, inositol- and choline- class (PS, PI and PC) and ceramide-phosphates (CerP) identified using an in-house lipid database (Reis et al., 2013, 2015).

The sulfate metabolome of biofluids and cell extracts shows a wide diversity of known SL structures as well as the presence of other sulfate-related compounds in fluids and cells not yet fully deciphered.

3.3. Semi-quantitation of SL in human fluids and cells

Fluid and cell extracts underwent the same extraction protocol (Folch protocol) and were diluted to the same concentration (25 ng PL/μL) prior to MS injection. The strategy to normalize lipid extracts to the same injected amount (ng PL/μL) facilitates the estimates of SL per μg PL and hence the comparison of SL content in samples. Semi-quantitation estimates conducted using the low and high mass calibration curve equations (described in Section 1.1) show striking differences regarding the amount of SL per μg of phospholipid in human fluids and cells (Fig. 4) evidencing the heterogeneous distribution of SL across human fluids and tissues. Estimates on the relative SL concentration are expressed in pmoles SL/μg PL (shown in Fig. 4A) reflecting the sulphur/phosphorous ratio in the samples analysed. Values obtained show that for a specific amount of phospholipids, saliva is particularly rich in sulfate-based lipids whereas plasma is poor in SL.

As fluids and cells contained different phospholipids content (data not shown), estimates on the absolute amounts of SL (expressed in nmoles SL/mL of sample) show that plasma and seminal fluid contain the highest amount of SL among fluids analysed (Fig. 4B). Data further corroborates the heterogenous distribution of SL across biofluids. Estimates on the content of CholS show that seminal fluid and epithelial cells are particularly rich and seem to act as reservoirs of CholS (Fig. 4C) whereas all other fluids and cells, including sub-populations of LDL, exhibited similar content of CholS. The similar content of CholS observed for native (LDL (+)) and electronegative LDL (LDL(-)) (Fig. 4C) suggests that other compounds may contribute to the negative charge in electronegative LDL (-).

4. Discussion

Analysis of sulfate-based lipids is challenging as they occur in

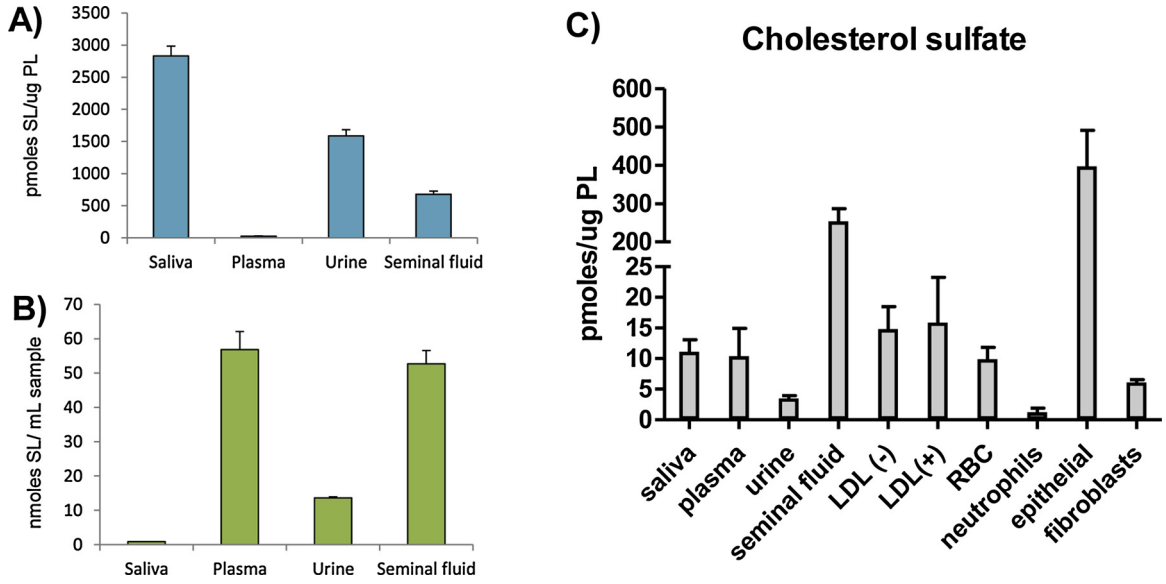

Fig. 4. Estimates of SL using calibration curves. (A) relative amount of SL per ug of phospholipid in extracts (pmoles SL/μg PL). (B) total amount of SL extracted from fluids (nmoles SL/mL sample). (C) Relative amount of cholesterol sulfate (pmoles/μg PL) in fluids and cell lipid extracts.

several sub-classes (Scheme 1) with a wide diversity of biochemical roles (Honke, 2018; Merten et al., 2001; Strott and Higashi, 2003). The presence of specific molecular traits in their structure (sulfate group) can be explored to design targeted approaches directed towards the specific detection of SL compounds with increased sensitivity even in complex mixtures. In fact, targeted MS-based approaches have been widely used for the SL detection but also due to their ability for structural characterization by tandem mass spectrometry (MS/MS) experiments. Despite the many studies conducted on the identification of SL in plasma (Lee et al., 2016; Mirzaian et al., 2015), saliva (Slomiany et al., 1988, 1983, 1978), urine (Yao et al., 2016), tear fluid (Lam et al., 2014), gastric fluid (Iwamori et al., 2000), seminal plasma (Sion et al., 2001), lipoproteins (Reis et al., 2013; Serna et al., 2015), red blood cells (Muskiet et al., 1983; Przybylska et al., 1995), blood platelets (Blache et al., 1995), and tissues brain (Moyano et al., 2013), kidney (Tadano-Aritomi et al., 2001), eye lenses (Seng et al., 2014), sperm cells (Fujimoto et al., 2000; Kongmanas et al., 2010; Zhang et al., 2005), hair (Cho et al., 2010; Drosche et al., 1994; Serizawa et al., 1990) and nails (Serizawa et al., 1990) and quantification by multi-reaction monitoring (MRM) (Fong et al., 2013; Kongmanas et al., 2010; Moyano et al., 2013; Sánchez-Guijo et al., 2015; Yao et al., 2016), these were mostly focused on specific steroid sulfates in individual fluids and cells (Esquivel et al., 2018; Fong et al., 2013; Lam et al., 2014; Przybylska et al., 1995; Sánchez-Guijo et al., 2015; Sion et al., 2001; Wang et al., 2018) leaving a whole panel of high Mw SL unaccounted for. In this study, the optimisation of targeted PIS 97 detection conditions to include low and high Mw SL (Figs. 1 and 2) revealed the presence of sulfate steroids, sulfoglycolipids, sulfated hypurate lipids, N-acyl taurine lipids and other unidentified sulfate lipid-based compounds identified in the same mass spectra (Fig. 3).

The mass spectra also revealed that SL are heterogeneously distributed across fluids and cell extracts (Fig. 3) with the presence of steroid sulfates in all extracts while sulfated glycolipids were found in saliva, blood and seminal plasma, urine in agreement with previously published literature (Blache et al., 1995; Fujimoto et al., 2000; Sánchez-Guijo et al., 2015; Slomiany et al., 1978; Yao et al., 2016). Because, PIS 97 mass spectra were acquired in lipid extracts with the same amount of phospholipids, then the intensity of SL ions observed in each PIS 97 mass spectra is comparable. Aside from SL, other sulfate-based lipids were also detected in biofluids and cell extracts including sulfated hypurate conjugates, N-acyl taurines, polyphenol metabolites, and other unidentified sulfate-related lipids (Table 1). Remarkably, sulfatides (sulfated glyco-sphingolipids) typically found in human fluids and tissues (Mirzaian et al., 2015; Moyano et al., 2013; Reis et al., 2013) were not detected in lipid extracts of biofluids and cells. The reasons behind this may be related to experimental, instrumental and physiological aspects. The extraction solvent system adopted (Folch method) was previously reported to extract > 95% of total sulfatides in plasma samples (Mirzaian et al., 2015) though more polar solvent systems proved to have higher extraction performances towards sphingolipids (Matyash et al., 2008) and may prove to be more efficient in the extraction of SL. Also, the CE value selected (−80 eV) was a compromise value between the optimum CE observed for low molecular weight SL and high molecular weight SL (Fig. 1A). Hence, the limitations associated with experimental and instrumental conditions used may have conditioned the detection of sulfatides in healthy fluids and tissues with reportedly sub-micromolar basal levels (Mirzaian et al., 2015), although may not compromise the detection of sulfatides in diseased samples characterized with higher levels of sulfatides (Spacil et al., 2016).

The semi-quantification estimates obtained in this study revealed a heterogenous distribution of SL across human fluids (Fig. 4A). Estimates of SL per μg PL conducted for the various extracts show that plasma exhibits the lowest sulphur-to-phosphorous ratio whereas seminal fluid, due to the abundance of seminolipids, exhibits the highest sulphur-to-phosphorous ratio. As the final estimates are affected by extraction performance, the use of different extraction methods and solvent systems during SL extracts sample preparation makes the comparison of the reported data more difficult. In our study, sample extracts were prepared using the same extraction protocol, and to account for the different phospholipid content in the various samples (data not shown) estimates were conducted using the same amount of phospholipid in the lipid extract. Taking these 2 aspects in consideration, the absolute amounts of SL in fluids (amount SL/mL) shows that plasma contains the highest absolute amount of SL (Fig. 4B).

Individually, CholS was detected in all fluid and cell extracts with particular abundance in seminal fluid and epithelial cells (Fig. 4C) whereas sulfated glycolipids were found in saliva and seminal fluid samples (Table 1). CholS is transported in circulation to peripheric tissues by lipoproteins (Reis et al., 2013, 2015) but remarkably, the content of CholS in native and electronegative LDL was very similar (Fig. 4C) suggesting that CholS and other SL may have a negligible

effect to the electronegativity of atherogenic LDL in normolipidemia. The increased charge of electronegative LDL(-) is due to a set of factors, including higher content of NEFA and minor apolipoproteins, as well as alterations in the structure of ApoB due to oxidation, glycation, carbamylation, desialization and possibly other causes that have not been fully described (Sánchez-Quesada et al., 2012). The high content of CholS observed for seminal plasma (Fig. 4C) may act as a substrate for intra-uterine enzymes and adhesion of sperm cells to the uterine wall. In the human cells, epidermal CholS is known to peak transiently during keratinocyte differentiation (Lampe et al., 1983) and to exert a crucial role in formation and function of the skin's permeability barrier (Elias et al., 2014). A powerful tool to quantify epidermal CholS is thus not only potentially useful in monitoring X-linked icthyosis therapy (where CholS levels are drastically dysregulated) but may also serve as a biomarker for epidermal barrier status for skin care- or therapeutic intervention.

While the presence of sulfoglycolipids in saliva is in accordance with earlier findings reported in the literature (Larsson et al., 1996; Slomiany et al., 1983, 1978), their content in saliva is still debatable ranging between 5% (Larsson et al., 1996) to 20–30% (Slomiany et al., 1988). Ions identified in saliva and seminal fluid as sulfoglycolipids were observed as odd-numbered ions and thus consistent with acylglycerol-based lipids (nitrogen rule) and in accordance with earlier works (Goto-Inoue et al., 2009; Kongmanas et al., 2010; Slomiany et al., 1983, 1978). The distinct structural difference reported between the sulfoglycolipids from saliva and seminal fluid refers to the sugar residue, with the presence of sulfo-glucosyl-(acylglycerol) lipids in saliva (Slomiany et al., 1978) and sulfo-galactosyl-(acylglycerol) lipids in semen (Kongmanas et al., 2010). The structural features concerning the sugar moiety and others concerning the fatty acyl composition (Kongmanas et al., 2010; Slomiany et al., 1978) may account for the biological roles of sulfoglycolipids in saliva and seminal plasma. Typically, mammalian fluids and cells contain sulfo-galactosyl-sphingosine lipids (sulfatides) (Quehenberger and Dennis, 2011) and although much is known on the role of sulfatides (Kyogashima, 2004; Suzuki et al., 2003), the biological role of sulfated glyco-glycerolipids found in saliva and seminal fluid (seminolipids) and their location remains poorly understood. Initial works by Slomiany's group in the 1980's revealed the presence of glucoglycerol-based lipids were key for proper hydrophobicity, viscosity and the number of binding sites pivotal to mucin´s function (Slomiany et al., 1989, 1983) and possibly in susceptibility to pathogen growth and oral defence (Slomiany et al., 1989). In saliva, sulfoglycolipids were found entangled in mucin´s network (Slomiany et al., 1989, 1983, 1978) but interestingly the presence of apoproteins identified in saliva (Huang, 2004; Wu et al., 2015) and seminal plasma proteome studies (Kumar et al., 2009) evidence the presence of lipoproteins in these fluids suggesting that the transport of sulfoglycolipids in saliva and seminal fluid occurs by lipoproteins similar in blood plasma. In a previous case-control study, Reis et al. (2015) reported the presence of sulfatides and cholesterol sulfate which were found in significantly lower levels in LDL from patients with chronic kidney disease. In overview, the biological role of endogenous sulfated glycerol-based glycolipids may be more exciting as recently structurally similar compounds extracted from marine algae exhibited antiviral activity against herpes simplex type-1 (Plouguerné et al., 2013) and reported as potent glutamyl cyclase inhibitors with potential to attenuate the effects of neurodegenerative diseases such as Alzheimer disease (Hielscher-Michael et al., 2016).

In addition to steroid sulfates and sulfoglycolipids, lipids containing the sulfuryl group (N-acyl taurines) were identified in plasma, neutrophils and epithelial cell extracts (Table 1). Taurine lipids are transported in circulation by plasma triglyceride-rich lipoproteins (Reis et al., 2015, 2013) and due to their amphipathic character may act as surfactants. In tissues, researchers noticed that local administration of synthetic N-acyl taurines (NATs) accelerated wound closure in mice and stimulated repair-associated responses in primary cultures of human keratinocytes and fibroblasts (Sasso et al., 2016) and to actively regulate differentiation of fibroblasts and mitogenesis in human keratinocytes (Sasso et al., 2016). In another study, several amino acid-based surfactants were evaluated to their *in vitro* skin permeation (Okasaka et al., 2018) where taurine-based surfactants exhibited an intermediate behaviour and a more biocompatible option to sulfate-based surfactants (i.e. SDS). Taurine-lipids were also proposed as fatty acid amid hydrolase (FAAH) inhibitors (Long et al., 2011; Saghatelian et al., 2006), anti-proliferative effect in prostate cancer cell line (Chatzakos et al., 2012); increase insulin secretion (Waluk et al., 2013) and activation of transient receptor potential (TRP) calcium channels (Saghatelian et al., 2006) supporting the need for additional screening studies in fluids and cells.

In view of the complexity of identified and unidentified SL in this study, the full knowledge of the panel, content and role endogenous SL remains elusive, and further studies aimed to complete the sulfur metabolome in fluids and cells are crucial.

The occurrence of specific structural features in biomolecules, such as the sulfate group, is advantageously explored in advanced mass spectrometers to design and fine-tunning sensitive detection methods thus improving the identification of residual compounds even in complex samples. The ability to acquire the fragmentation pattern, render QTrap instruments increased versatility and popularity in metabolite profiling. Nevertheless, it should be noted that due to specific acquisition settings and instrumental limitations associated with QTrap instruments, the complete panel of SL and sulfated conjugates in human biofluids and cells is likely to be greater than the one here reported. For instance, in this study the mass range parameter was set at m/z 350 so that low molecular weight SL (< 350 Da) with greater ionization efficiency would not suppress the detection of less ionizable with higher molecular weight SL. In addition, QTrap MS instruments have fixed mass scan range limited to m/z 1000 meaning that high molecular weight SL (> 1000 Da) are not detected. Also, due to the scarcity of synthetic standards, only 2 calibration curves built in the low-mass and high-mass region were used which poses limitations with the approach adopted in this study. Nevertheless, estimates conducted on human fluid and cell lipid extracts prepared using the same protocol (Folch extraction) and normalized to the same phospholipids amount provides an evaluation of the sulfur-to-phosphorous ratio never conducted before. The sulfur-to-phosphorous ratio in biofluids and cells reflects the interplay of sulfotransferases/sulfatases enzymes in biochemical and physiological processes evidencing that sulfotransferase/sulfatase enzymes may have a more relevant role in human physiology and pathophysiology, particularly as SULT may also be involved in detoxification of cytotoxic oxidised lipids (oxysterols) (Fuda et al., 2007) and required for proper lipoprotein clearance (Stanford et al., 2010) as already proposed opening exciting new avenues in cardiovascular, testicular aging and fertility, skin aging and wound healing, and oncology areas.

5. Concluding remarks

Based on the results described here it is clear that the human sulfateome (sulfate metabolome) of human fluids and cells is complex with a wide diversity of sulfate-based lipids and is not restricted to steroid sulfates and sulfoglycolipids, as it includes other unidentified SL compounds as part of the complex human metabolome. Our results highlight the need to expand the panel of synthetic commercial standards to include compounds (in the low- and high mass region) with these molecular traits for accurate quantification.

The standardization of lipid extraction step with the same solvent system for all fluids, operating in the same MS instrument minimized variations in SL estimates due to dissimilar extraction performances associated with LLE procedures. Estimates conducted with lipid extracts normalized to the same phospholipid amount provides an evaluation of the sulfur-to-phosphorous ratio in the human fluids and cells which has

been done in this study for the first time. It is encouraged that researchers adopt this approach in future studies as it will consider variations that may occur during the extraction step if other solvent systems are selected.

Given the attractiveness of non-invasive and minimally invasive fluids in disease diagnostics it is crucial to include analyses with higher sample size in future biological samples in order to fully understand the panel, distribution and levels of SL in health and monitor changes on SL that may occur with age, gender, and ethnicity. Likewise, inclusion of other minimally invasive fluids (breast milk, tear fluid, sweat) or to more relevant invasive biofluids (amniotic fluid, synovial fluid, cerebrospinal fluid, and pericardial fluid) in the screening of SL in biomarker discovery will not only complete the metabolome panel of biofluids but will likely be an additional tool in disease prediction, diagnosis, stratification and therapeutic prognosis.

Conflict of interests

The authors declare no conflict of interests.

Author´s contributions

AR conceived and designed the study; ID, RF, FG, RV, MF, JV, ARU, JLQ were involved in sample collection and sample processing. AR conducted lipid extraction and Pi quantification; ID performed the MS experiments; AR analyzed the data; AR and ID were involved in drafting and writing the manuscript; all authors were involved in the critical revising the manuscript. All authors have approved the final version.

Acknowledgements

HKID acknowledges support from Kidney Research Foundation PDF3/2014. HKID and AR also acknowledge visiting researcher funds received from Life and Health Sciences, Aston University. AR gratefully acknowledges funding from Portuguese National Funds (NORTE-01-0145-FEDER-000011). RF acknowledges the QOPNA (UID/QUI/00062/2013). The financial support for FG by the Austrian Federal Ministry for Digital and Economic Affairs and the Austrian National Foundation for Research, Technology and Development is gratefully acknowledged. MF acknowledges the support of FEDER funds through the “Programa Operacional Competitividade e Internacionalização-COMPETE 2020” and the National Funds through the FCT- Fundação para a Ciência e Tecnologia, JLS-Q acknowledges support from ISCIII-FIS PI16-00471 and CIBERDEM. Projects PTDB/BBB-BQB/3804/2014. RV, MF and JVS are thankful to iBiMED (UID/BIM/04501/2013 and POCI-01-0145-FEDER-007628) for supporting this project. This work was also supported by an individual grant from FCT to JVS (SFRH/BPD/123155/2016).

Appendix A. Supplementary data

Supplementary material related to this article can be found, in the online version, at doi:https://doi.org/10.1016/j.chemphyslip.2019.03.009.

References

Avila, J.L., Rojas, M., Avila, A., 1996. Cholesterol sulphate-reactive autoantibodies are specifically increased in chronic chagasic human patients. Clin. Exp. Immunol. 103, 40–46.

Bancells, C., Villegas, S., Blanco, F.J., Benítez, S., Gállego, I., Beloki, L., Pérez-Cuellar, M., Ordóñez-Llanos, J., Sánchez-Quesada, J.L., 2010. Aggregated electronegative low density lipoprotein in human plasma shows a high tendency toward phospholipolysis and particle fusion. J. Biol. Chem. 285, 32425–32435.

Blache, D., Becchi, M., Davignom, J., 1995. Occurence and biological effects of cholesteryl sulfate on blood platelets. Biochim. Biophys. Acta 1259, 291–296.

Chatzakos, V., Slätis, K., Djureinovic, T., Helleday, T., Hunt, M.C., 2012. N-acyl taurines are anti-proliferative in prostate cancer cells. Lipids 47, 355–361.

Cho, S.H., Choi, M.H., Sim, W.Y., Lee, W.Y., Chung, B.C., 2010. Metabolic alterations of DHEA and cholesterol sulphates in the hair of patients with acne measured by liquid chromatography-mass spectrometry. Exp. Dermatol. 19, 694–696.

Drosche, T., Gollwitzer, J., Platt, D., 1994. Cholesterol and cholesterol sulfate concentration in the cell membrane complex of human scalp hair. Arch. Gerontol. Geriatr. 4, 19–30.

Eberlin, L.S., Dill, A.L., Costa, A.B., Ifa, D.R., Cheng, L., Masterson, T., Koch, M., Ratliff, T.L., Cooks, R.G., 2010. Letters to Analytical Chemistry Cholesterol Sulfate Imaging in Human Prostate Cancer Tissue by Desorption Electrospray Ionization Mass Spectrometry. Anal. Chem. 82, 3430–3434.

Elias, P.M., Williams, M.L., Choi, E.H., Feingold, K.R., 2014. Role of cholesterol sulfate in epidermal structure and function: lessons from X-linked ichthyosis. Biochim. Biophys. Acta - Mol. Cell Biol. Lipids 1841, 353–361.

Esquivel, A., Alechaga, É., Monfort, N., Ventura, R., 2018. Direct quantitation of endogenous steroid sulfates in human urine by liquid chromatography-electrospray tandem mass spectrometry. Drug Test. Anal.

Farooqui, A.A., Horrocks, L.A., 1985. Roles of sulfolipids in metabolism. II. Mol. Cell. Biochem. 95, 87–95.

Fenn, J.B., Mann, M., Meng, C.K., Wong, S.F., Whitehouse, C.M., 1989. Electrospray ionization for mass spectrometry of large biomolecules. Science 246, 64–71.

Folch, J., Lees, M., Sloane Stanley, G.H., 1957. A simple method for the isolation and purification of total lipides from animal tissues. J. Biol. Chem. 226, 497–509.

Fong, B.M.W., Tam, S., Leung, K.S.Y., 2013. Determination of plasma cholesterol sulfate by LC-APCI-MS/MS in the context of pediatric autism. Talanta 116, 115–121.

Fuda, H., Javitt, N.B., Mitamura, K., Ikegawa, S., Strott, C.A., 2007. Oxysterols are substrates for cholesterol sulfotransferase. J. Lipid Res. 48, 1343–1352.

Fujimoto, H., Tadano-Aritomi, K., Tokumasu, A., Ito, K., Hikita, T., Suzuki, K., Ishizuka, I., 2000. Requirement of seminolipid in spermatogenesis revealed by UDP-galactose: ceramide galactosyltransferase-deficient mice. J. Biol. Chem. 275, 22623–22626.

Garwolińska, D., Hewelt-Belka, W., Namieśnik, J., Kot-Wasik, A., 2017. Rapid characterization of the human breast milk lipidome using a solid-phase microextraction and liquid chromatography-mass spectrometry-based approach. J. Proteome Res. 16, 3200–3208.

Goldberg, I.H., 1961. The sulfolipids. J. Lipid Res. 2, 103–109.

Goto-Inoue, N., Hayasaka, T., Zaima, N., Setou, M., 2009. The specific localization of seminolipid molecular species on mouse testis during testicular maturation revealed by imaging mass spectrometry. Glycobiology 19, 950–957.

Gruber, F., Oskolkova, O., Leitner, A., Mildner, M., Mlitz, V., Lengauer, B., Kadl, A., Mrass, P., Krönke, G., Binder, B.R., Bochkov, V.N., Leitinger, N., Tschachler, E., 2007. Photooxidation generates biologically active phospholipids that induce heme oxygenase-1 in skin cells. J. Biol. Chem. 282, 16934–16941.

Gruber, F., Bicker, W., Oskolkova, O.V., Tschachler, E., Bochkov, V.N., 2012. A simplified procedure for semi-targeted lipidomic analysis of oxidized phosphatidylcholines induced by UVA irradiation. J. Lipid Res. 53, 1232–1242.

Hammond, V.J., Morgan, A.H., Lauder, S., Thomas, C.P., Brown, S., Freeman, B.A., Lloyd, C.M., Davies, J., Bush, A., Levonen, A.L., Kansanen, E., Villacorta, L., Chen, Y.E., Porter, N., Garcia-Diaz, Y.M., Schopfer, F.J., O'Donnell, V.B., 2012. Novel ketophospholipids are generated by monocytes and macrophages, detected in cystic fibrosis, and activate peroxisome proliferator-activated receptor-γ. J. Biol. Chem. 287, 41651–41666.

Hart, P.J., Francese, S., Claude, E., Woodroofe, M.N., Clench, M.R., 2011. MALDI-MS imaging of lipids in ex vivo human skin. Anal. Bioanal. Chem. 401, 115–125.

Hielscher-Michael, S., Griehl, C., Buchholz, M., Demuth, H.U., Arnold, N., Wessjohann, L.A., 2016. Natural products from microalgae with potential against Alzheimer's disease: sulfolipids are potent glutaminyl cyclase inhibitors. Mar. Drugs 14, 203–219.

Hofmann, T., Nebehaj, E., Albert, L., 2016. Antioxidant properties and detailed polyphenol profiling of European hornbeam (Carpinus betulus L.) leaves by multiple antioxidant capacity assays and high-performance liquid chromatography/multistage electrospray mass spectrometry. Ind. Crops Prod. 87, 340–349.

Honke, K., 2018. Biological functions of sulfoglycolipids and the EMARS method for identification of co-clustered molecules in the membrane microdomains. J. Biochem. 163, 253–263.

Hsu, F.F., Turk, J., 2003. Electrospray ionization/tandem quadrupole mass spectrometric studies on phosphatidylcholines: the fragmentation processes. J. Am. Soc. Mass Spectrom. 14, 352–363.

Hu, R., Li, G., Kamijo, Y., Aoyama, T., Nakajima, T., Inoue, T., Node, K., Kannagi, R., Kyogashima, M., Hara, A., 2007. Serum sulfatides as a novel biomarker for cardiovascular disease in patients with end-stage renal failure. Glycoconj. J. 24, 565–571.

Huang, C.M., 2004. Comparative proteomic analysis of human whole saliva. Arch. Oral Biol. 49, 951–962.

Iwamori, M., Suzuki, H., Kimura, T., Iwamori, Y., 2000. Shedding of sulfated lipids into gastric fluid and inhibition of pancreatic DNase I by cholesterol sulfate in concert with bile acids. Biochim. Biophys. Acta - Mol. Cell Biol. Lipids 1487, 268–274.

Karas, M., Bachmann, D., Bahr, U., Hillenkamp, F., 1987. Matrix-assisted ultraviolet laser desorption of non-volatile compounds. Int. J. Mass Spectrom. Ion Process. 78, 53–68.

Kompauer, M., Heiles, S., Spengler, B., 2017. Atmospheric pressure MALDI mass spectrometry imaging of tissues and cells at 1. 4- um lateral resolution. Nat. Methods 14, 90–96.

Kongmanas, K., Xu, H., Yaghoubian, A., Franchini, L., Panza, L., Ronchetti, F., Faull, K., Tanphaichitr, N., 2010. Quantification of seminolipid by LC-ESI-MS/MS-multiple reaction monitoring: compensatory levels in Cgt(+/−) mice. J. Lipid Res. 51, 3548–3558.

Kosinska, M.K., Liebisch, G., Lochnit, G., Wilhelm, J., Klein, H., Kaesser, U., Lasczkowski, G., Rickert, M., Schmitz, G., Steinmeyer, J., 2013. A lipidomic study of phospholipid classes and species in human synovial fluid. Arthritis Rheum. 65, 2323–2333.

Kumar, V., Hassan, M.I., Tomar, A.K., Kashav, T., Nautiyal, J., Singh, S., Singh, T.P.,

Yadav, S., 2009. Proteomic analysis of heparin-binding proteins from human seminal plasma: a step towards identification of molecular markers of male fertility. J. Biosci. 34, 899–908.
Kyogashima, M., 2004. The role of sulfatide in thrombogenesis and haemostasis. Arch. Biochem. Biophys. 426, 157–162.
Lafaye, A., Junot, C., Ramounet-Le Gall, B., Fritsch, P., Ezan, E., Tabet, J.C., 2004. Profiling of sulfoconjugates in urine by using precursor ion and neutral loss scans in tandem mass spectrometry. Application to the investigation of heavy metal toxicity in rats. J. Mass Spectrom. 39, 655–664.
Lam, S.M., Tong, L., Reux, B., Duan, X., Petznick, A., Yong, S.S., Khee, C.B.S., Lear, M.J., Wenk, M.R., Shui, G., 2014. Lipidomic analysis of human tear fluid reveals structure-specific lipid alterations in dry eye syndrome. J. Lipid Res. 55, 299–306.
Lampe, Ma, Williams, M.L., Elias, P.M., 1983. Human epidermal lipids: characterization and modulations during differentiation. J. Lipid Res. 24, 131–140.
Larsson, B., Olivecrona, G., Ericson, T., 1996. Lipids in human saliva. Arch. Oral Biol. 41, 105–110.
Lee, D.Y., Kind, T., Yoon, Y.R., Fiehn, O., Liu, K.H., 2014. Comparative evaluation of extraction methods for simultaneous mass-spectrometric analysis of complex lipids and primary metabolites from human blood plasma. Anal. Bioanal. Chem. 406, 7275–7286.
Lee, S.H., Lee, N., Hong, Y., Chung, B.C., Choi, M.H., 2016. Simultaneous analysis of free and sulfated steroids by liquid chromatography/mass spectrometry with selective mass spectrometric scan modes and polarity switching. Anal. Chem. 88, 11624–11630.
Leitinger, N., Tyner, T.R., Oslund, L., Rizza, C., Subbanagounder, G., Lee, H., Shih, P.T., Mackman, N., Tigyi, G., Territo, M.C., Berliner, Ja, Vora, D.K., 1999. Structurally similar oxidized phospholipids differentially regulate endothelial binding of monocytes and neutrophils. Proc. Natl. Acad. Sci. U. S. A. 96, 12010–12015.
Liu, Y., Chen, Y., Momin, A., Shaner, R., Wang, E., Bowen, N.J., Matyunina, L.V., Walker, L.D., McDonald, J.F., Sullards, M.C., Merrill Jr., A.H., 2010. Elevation of sulfatides in ovarian cancer: an integrated transcriptomic and lipidomic analysis including tissue-imaging mass spectrometry. Mol. Cancer 9, 186.
Long, J.Z., LaCava, M., Jin, X., Cravatt, B.F., 2011. An anatomical and temporal portrait of physiological substrates for fatty acid amide hydrolase. J. Lipid Res. 52, 337–344.
Maciel, E., Neves, B.M., Santinha, D., Reis, A., Domingues, P., Teresa Cruz, M., Pitt, A.R., Spickett, C.M., Domingues, M.R.M., 2014. Detection of phosphatidylserine with a modified polar head group in human keratinocytes exposed to the radical generator AAPH. Arch. Biochem. Biophys. 548, 38–45.
Masterson, T.A., Dill, A.L., Eberlin, L.S., Mattarozzi, M., Cheng, L., Beck, S.D.W., Bianchi, F., Cooks, R.G., 2011. Distinctive glycerophospholipid profiles of human seminoma and adjacent normal tissues by desorption electrospray ionization imaging mass spectrometry. J. Am. Soc. Mass Spectrom. 22, 1326–1333.
Matthews, J.B., Wright, H.J., Roberts, A., Cooper, P.R., Chapple, I.L.C., 2007. Hyperactivity and reactivity of peripheral blood neutrophils in chronic periodontitis. Clin. Exp. Immunol. 147, 255–264.
Matyash, V., Liebisch, G., Kurzchalia, T.V., Shevchenko, A., Schwudke, D., 2008. Lipid extraction by methyl-tert-butyl ether for high-throughput lipidomics. J. Lipid Res. 49, 1137–1146.
Merten, M., Dong, J.F., Lopez, J.A., Thiagarajan, P., 2001. Cholesterol sulfate: a new adhesive molecule for platelets. Circulation 103, 2032–2034.
Metzger, K., Erben, G., Lehmann, W.D., Rehberger, P.A., 1995. Identification and quantification of lipid sulfate esters by electrospray ionization MS/MS techniques: cholesterol sulfate. Anal. Chem. 67, 4178–4183.
Mirzaian, M., Kramer, G., Poorthuis, B.J.H.M., 2015. Quantification of sulfatides and lysosulfatides in tissues and body fluids by liquid chromatography-tandem mass spectrometry. J. Lipid Res. 56, 936–943.
Moyano, A.L., Pituch, K., Li, G., Van Breemen, R., Mansson, J.E., Givogri, M.I., 2013. Levels of plasma sulfatides C18: 0 and C24: 1 correlate with disease status in relapsing-remitting multiple sclerosis. J. Neurochem. 127, 600–604.
Moyano, A.L., Li, G., Lopez-Rosas, A., Månsson, J.-E., van Breemen, R.B., Givogri, M.I., 2014. Distribution of C16:0, C18:0, C24:1, and C24:0 sulfatides in central nervous system lipid rafts by quantitative ultra-high-pressure liquid chromatography tandem mass spectrometry. Anal. Biochem. 467, 31–39.
Muskiet, F.A., Jansen, G., Wolthers, B.G., Marinkovic-Ilsen, A., van Voorst Vader, P.C., 1983. Gas-chromatographic determination of cholesterol sulfate in plasma and erythrocytes, for the diagnosis of recessive X-linked ichthyosis. Clin. Chem. 29, 1404–1407.
Okasaka, M., Kubota, K., Yamasaki, E., Yang, J., Takata, S., 2018. Evaluation of anionic surfactants effects on the skin barrier function based on skin permeability. Pharm. Dev. Technol. 0, 1–6.
Pizarro, C., Arenzana-Rámila, I., Pérez-Del-Notario, N., Pérez-Matute, P., González-Sáiz, J.M., 2013. Plasma lipidomic profiling method based on ultrasound extraction and liquid chromatography mass spectrometry. Anal. Chem. 85, 12085–12092.
Plouguerné, E., De Souza, L.M., Sassaki, G.L., Cavalcanti, J.F., Romanos, M.T.V., Da Gama, B.A.P., Pereira, R.C., Barreto-Bergter, E., 2013. Antiviral sulfoquinovosyldiacylglycerols (SQDGs) from the Brazilian brown seaweed Sargassum vulgare. Mar. Drugs 11, 4628–4640.
Przybylska, M., Bryszewska, M., Nowicka, U., Szosland, K., Kędziora, J., Epand, R.M., 1995. Estimation of cholesterol sulphate in blood plasma and in erythrocyte membranes from individuals with Down's syndrome or diabetes mellitus type I. Clin. Biochem. 28, 593–597.
Quehenberger, O., Dennis, E.A., 2011. The human plasma lipidome. N. Engl. J. Med. 365, 1812–1823.
Reis, A., Rudnitskaya, A., Blackburn, G.J., Mohd Fauzi, N., Pitt, A.R., Spickett, C.M., 2013. A comparison of five lipid extraction solvent systems for lipidomic studies of human LDL. J. Lipid Res. 54, 1812–1824.
Reis, A., Rudnitskaya, A., Chariyavilaskul, P., Dhaun, N., Melville, V., Goddard, J., Webb, D.J., Pitt, A.R., Spickett, C.M., 2015. Top-down lipidomics of low density lipoprotein reveal altered lipid profiles in advanced chronic kidney disease. J. Lipid Res. 56, 413–422.
Rouser, G., Fleischer, S., Yamamoto, A., 1970. Two dimensional thin layer chromatographic separation of polar lipids and determination of phospholipids by phosphorus analysis of spots. Lipids 5, 494–496.
Saghatelian, A., McKinney, M.K., Bandell, M., Patapoutian, A., Cravatt, B.F., 2006. A FAAH-regulated class of N-acyl taurines that activates TRP ion channels. Biochemistry 45, 9007–9015.
Sánchez-Guijo, A., Oji, V., Hartmann, M.F., Traupe, H., Wudy, S.A., 2015. Simultaneous quantification of cholesterol sulfate, androgen sulfates, and progestagen sulfates in human serum by LC-MS/MS. J. Lipid Res. 56, 1843–1851.
Sánchez-Quesada, J.L., Villegas, S., Ordóñez-Llanos, J., 2012. Electronegative low-density lipoprotein. A link between apolipoprotein B misfolding, lipoprotein aggregation and proteoglycan binding. Curr. Opin. Lipidol. 23, 479–486.
Sarafian, M.H., Gaudin, M., Lewis, M.R., Martin, F.-P., Holmes, E., Nicholson, J.K., Dumas, M.-E., 2014. Objective set of criteria for optimization of sample preparation procedures for ultra-high throughput untargeted blood plasma lipid profiling by ultra performance liquid chromatography – mass spectrometry. Anal. Chem. 86, 5766–5774.
Sasso, O., Pontis, S., Armirotti, A., Cardinali, G., Kovacs, D., Migliore, M., Summa, M., Moreno-Sanz, G., Picardo, M., Piomelli, D., 2016. Endogenous *N* -acyl taurines regulate skin wound healing. Proc. Natl. Acad. Sci. 113, E4397–E4406.
Satoh Née Okihara, R., Saito, T., Ogata, H., Ohsaki, A., Iida, T., Asahina, K., Mitamura, K., Ikegawa, S., Hofmann, A.F., Hagey, L.R., 2014. N-Methyltaurine N-acyl amidated bile acids and deoxycholic acid in the bile of angelfish (Pomacanthidae): a novel bile acid profile in Perciform fish. Steroids 80, 15–23.
Schuhmann, K., Almeida, R., Baumert, M., Herzog, R., Bornstein, S.R., Shevchenko, A., 2012. Shotgun lipidomics on a LTQ Orbitrap mass spectrometer by successive switching between acquisition polarity modes. J. Mass Spectrom. 47, 96–104.
Seng, J.A., Ellis, S.R., Hughes, J.R., Maccarone, A.T., Truscott, R.J.W., Blanksby, S.J., Mitchell, T.W., 2014. Characterisation of sphingolipids in the human lens by thin layer chromatography-desorption electrospray ionisation mass spectrometry. Biochim. Biophys. Acta 1841, 1285–1291.
Serizawa, S., Nagai, T., Ito, M., Sato, Y., 1990. Cholesterol sulphate levels in the hair and nails of patients with recessive X-linked ichthyosis. Clin. Exp. Dermatol. 15, 13–15.
Serna, J., García-Seisdedos, D., Alcázar, A., Lasunción, M.Á., Busto, R., Pastor, Ó., 2015. Quantitative lipidomic analysis of plasma and plasma lipoproteins using MALDI-TOF mass spectrometry. Chem. Phys. Lipids 189, 7–18.
Sion, B., Grizard, G., Boucher, D., 2001. Quantitative analysis of desmosterol, cholesterol and cholesterol sulfate in semen by high-performance liquid chromatography. J. Chromatogr. A 935, 259–265.
Slomiany, B.L., Slomiany, A., Glass, G.B.J., 1978. Glyceroglucolipids of the human saliva. Eur. J. Biochem. 84, 53–59.
Slomiany, B.L., Witas, H., Murty, V.L., Slomiany, a, Mandel, I.D., 1983. Association of lipids with proteins and glycoproteins in human saliva. J. Dent. Res. 62, 24–27.
Slomiany, B.L., Murty, V., Sarosiek, J., Piotrowski, J., Slomiany, A., 1988. Role of associated and covalently bound lipids in salivary mucin hydrophobicity: effect of proteolysis and disulfide bridge reduction. Biochem. Biophys. Res. Commun. 151, 1046–1053.
Slomiany, B.L., Murty, V.L.N., Mandel, I.D., Zalesna, G., Slomiany, A., 1989. Physicochemical characteristics of mucus glycoproteins and lipids of the human oral mucosal mucus coat in relation to caries susceptibility. Arch. Oral Biol. 34, 229–237.
Sousa, B., Melo, T., Campos, A., Moreira, A.S.P., Maciel, E., Domingues, P., Carvalho, R.P., Rodrigues, T.R., Girão, H., Domingues, M.R.M., 2016. Alteration in phospholipidome profile of myoblast H9c2 cell line in a model of myocardium starvation and ischemia. J. Cell. Physiol. 231, 2266–2274.
Spacil, Z., Babu Kumar, A., Liao, H.-C., Auray-Blais, C., Stark, S., Suhr, T.R., Scott, C.R., Turecek, F., Gelb, M.H., 2016. Sulfatide analysis by mass spectrometry for screening of metachromatic leukodystrophy in dried blood and urine samples. Clin. Chem. 62, 279–286.
Stanford, K.I., Wang, L., Castagnola, J., Song, D., Bishop, J.R., Brown, J.R., Lawrence, R., Bai, X., Habuchi, H., Tanaka, M., Cardoso, W.V., Kimata, K., Esko, J.D., 2010. Heparan sulfate 2-O-sulfotransferase is required for triglyceride-rich lipoprotein clearance. J. Biol. Chem. 285, 286–294.
Strott, C.A., Higashi, Y., 2003. Cholesterol sulfate in human physiology: what's it all about? J. Lipid Res. 44, 1268–1278.
Stübiger, G., Aldover-Macasaet, E., Bicker, W., Sobal, G., Willfort-Ehringer, A., Pock, K., Bochkov, V., Widhalm, K., Belgacem, O., 2012. Targeted profiling of atherogenic phospholipids in human plasma and lipoproteins of hyperlipidemic patients using MALDI-QIT-TOF-MS/MS. Atherosclerosis 224, 177–186.
Suzuki, T., Takahashi, T., Nishinaka, D., Murakami, M., Fujii, S., Hidari, K.I., Miyamoto, D., Li, Y.T., Suzuki, Y., 2003. Inhibition of influenza A virus sialidase activity by sulfatide. FEBS Lett. 553, 355–359.
Tadano-Aritomi, K., Hikita, T., Suzuki, a, Toyoda, H., Toida, T., Imanari, T., Ishizuka, I., 2001. Determination of lipid-bound sulfate by ion chromatography and its application to quantification of sulfolipids from kidneys of various mammalian species. J. Lipid Res. 42, 1604–1608.
Teubel, J., Wüst, B., Schipke, C.G., Peters, O., Parr, M.K., 2018. Methods in endogenous steroid profiling – a comparison of gas chromatography mass spectrometry (GC–MS) with supercritical fluid chromatography tandem mass spectrometry (SFC-MS/MS). J. Chromatogr. A 1554, 101–116.
Waluk, D.P., Vielfort, K., Derakhshan, S., Aro, H., Hunt, M.C., 2013. N-Acyl taurines trigger insulin secretion by increasing calcium flux in pancreatic β-cells. Biochem. Biophys. Res. Commun. 430, 54–59.

Wang, R., Tiosano, D., Sánchez-Guijo, A., Hartmann, M.F., Wudy, S.A., 2018. Characterizing the steroidal milieu in amniotic fluid of mid-gestation: a LC–MS/MS study. J. Steroid Biochem. Mol. Biol.

Weerachatyanukul, W., Probodh, I., Kongmanas, K., Tanphaichitr, N., Johnston, L.J., 2007. Visualizing the localization of sulfoglycolipids in lipid raft domains in model membranes and sperm membrane extracts. Biochim. Biophys. Acta Biomembr. 1768, 299–310.

Wijeyesekera, A., Clarke, P., Bictash, M., Brown, I., Fidock, M., Ryckmans, T., Yap, I., Chan, Q., Stamler, J., Elliot, P., Holmes, E., Nicholson, J., 2012. Quantitative UPLC-MS/MS analysis of the gut microbial co-metabolites phenylacetylglutamine, 4-cresyl sulfate and hyppurate in human urine: INTERMAP study. Anal. Methods 4, 65–72.

Wu, C.C., Chu, H.W., Hsu, C.W., Chang, K.P., Liu, H.P., 2015. Saliva proteome profiling reveals potential salivary biomarkers for detection of oral cavity squamous cell carcinoma. Proteomics 15, 3394–3404.

Yao, Y., Wang, P., Shao, G., Del Toro, L.V.A., Codero, J., Giese, R.W., 2016. Nontargeted analysis of the urine nonpolar sulfateome: a pathway to the nonpolar xenobiotic exposome. Rapid Commun. Mass Spectrom. 30, 2341–2350.

Zhang, Y., Hayashi, Y., Cheng, X., Watanabe, T., Wang, X., Taniguchi, N., Honke, K., 2005. Testis-specific sulfoglycolipid, seminolipid, is essential for germ cell function in spermatogenesis. Glycobiology 15, 649–654.